A SEMI-EMPIRICAL MODEL OF RAIN ATTENUATION AT KA-BAND IN NORTHERN TAIWAN

K.-S. Chen [†] and **C.-Y. Chu**

Communication System Research Research
National Central University, Chung-Li, Taiwan

Y.-C. Tzeng

Department of Electronic Engineering
National United University, Maio-Li, Taiwan

Abstract—Combining a two-year measurement and numerical approach, a semi-empirical model has been developed for prediction of rain attenuation at Ka-band in northern Taiwan. This was done using the drop size distribution (DSD) measurement and the extinction coefficient calculated by T-matrix, followed by regressing with rain attenuation measurements in all seasons. The attenuation due to rain can be estimated by calculating the extinction coefficient over all of the rain drops within the antenna beam volume. Comparing with the measured data demonstrates that the proposed model proves sufficiently accurate for Ka-band signal attenuation in site specific. For purpose of cross reference, we also compared the proposed model with Crane and ITU-R-P838 rain attenuation models. The RMS error and chi-square test shows that the proposed semi-empirical model has better performance to predicted rain attenuation than Crane and ITU-RP383 models, implied that both model predictions may not be quite reliable in some specific areas. Analysis suggests that seasonal effects are strong in signal attenuation due to rain types. It means that rain rate itself is not a quite reliable enough to be the single parameter in the rain attenuation model.

1. INTRODUCTION

Attenuation due to rain restricts the system performance of radio communication and to some extents limits the usage of higher frequencies for terrestrial point-to-point microwave links and satellite communications [1–3]. Therefore, it poses an interesting and long term research topic. Extensive researches indicate that the specific rain attenuation is greatly dependent on the rain drop size distribution (DSD) that is closely related to the rain rate. As a matter of fact, DSD affects more directly the signal attenuation than rain rate itself, although the later has been more readily available in line of data recordings in meteorology and weather stations. The variability of DSD in different climatic zones, particularly in the subtropical and the tropical region, has been a major concern in developing the rain attenuation model on a global basis [4–11]. By measuring the DSD in India, Maitra [12] reports a very significant variability in the rain attenuation distribution and suggests the need of long term and extensive measurement of DSD in the tropical region. Recent study by Townsend et al. [13] explained the differences between measured and modeled attenuation that can partly be explained by uncertainty in the raindrop size distribution. They also suggest that a more elaborate scheme might attempt to estimate numerical values of the DSD parameters. A preliminary analysis of spatial variability of raindrop size distributions during stratiform rain events was carried out by Lee et al. [14]. It was found that the correlation of rainfall estimate error is higher than that of estimated rainfall rate and of rainfall rate calculated from DSDs. Scaling effects on DSD variability was also investigated by Berne et al. [15] in order to improve the understanding of the DSD variability at small spatial scales. The DSD reflects the microphysical processes at work in the clouds and during the fall of raindrops. However, DSD is a highly spatio-temporal dependent variable. All these important studies points that when applying or establishing the prediction models it is critical to consider the climate zone in order to better predict the rain attenuation from the rainfall rate data. This is because rainfall types and so is DSD are dependent on climate environments even with the same rain rate. Olsen et al. [16] discussed the path diversity of EM wave propagation on theoretical basis. Li et al. [17, 18] studied the scattering characteristics of the varying distorted raindrops to understand the effects of the large-scale raindrop distortion. The two-year experimental data of the rainfall attenuation of CW microwaves in Singapore were compared with the predicted specific attenuation computed by using the local raindrop size distribution. In [19], numerical solution on volume integral

equation formulation (VIEF) was used to calculate the scattering and absorption cross sections by raindrops to improve the theoretical model of EM wave which propagated through water particles. These researches are based on relationship between total volume extinction coefficient, drop size distribution, and single particle extinction factor. The single particle extinction factor often made use of EM wave scattering theory through spheroid or ellipsoid particle [3, 15].

From this aspect, this study presents 28 GHz rain attenuation by measuring DSD at different seasons in Taiwan [20] and subsequently takes them into account for the extinction calculation by T-matrix method. Then the rain attenuation prediction model was established and validated by in situ measurements.

2. DROP SIZE DISTRIBUTION OBSERVATION

It is note that for a given drop size D, the rain rate can be calculated by

$$R = 6\pi \times 10^{-4} \int_0^\infty D^3 v(D) N(D) dD \qquad (1)$$

Hence, it is essential to obtain the DSD information. By noting that the DSD excises more directly impacts on estimation and prediction of rain attenuation where the total extinction cross section was calculated using T-matrix approach [21]. Two 2D-Video distrometers were used to collect DSD data over Northern Taiwan in An Ken (24°57'32.46"N, 121°31'28.87"E) and Chung-Li (24°58'3.97"N, 121°11'6.55"E) at every 1 min at different seasons for two years, then the relation between the rain rate and DSD was established based on a power-law relationship ($y = aR^b$, y is mean or standard deviation of the DSD; R being the rain rate) that is subsequently used in estimation of rain attenuation at Ka-band. Regression fit was performed to match the data to widely known distributions: Gamma, Lognormal, and Weibull. It is found that Gamma model gives the best fit regardless of seasons [20]. The Gamma DSD model can be given as

$$N(D) = N_0 \frac{\lambda^\gamma}{\Gamma(\gamma)} D^{\gamma-1} e^{-\lambda D}$$
$$= \mu \frac{\gamma}{\lambda}, \quad \sigma^2 = \frac{\gamma}{\lambda^2} \qquad (2)$$

where $N(D)dD$ is the number density of drops between diameters D and $D+dD$. Three parameters to be determined in Eq. (2) are μ: mean, σ: standard deviation and N_0 is the rain drop numbers per unit volume, i.e., number density. Using the power-law to fit and

considering the minimum RMS for criteria, μ and σ can be obtained from the probability density function of the measurement data:

$$\mu = 0.6736R^{0.1947} \tag{3a}$$

$$\sigma = 0.2346R^{0.2935} \tag{3b}$$

where R is the rain rate in mm/hr.
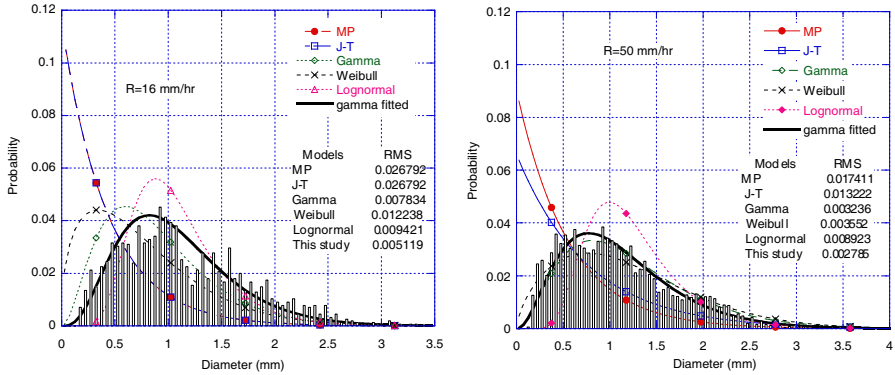
Figure 1. Probability density function of the raindrop diameter. Various models are plotted, along with the gamma fitted in this study which shows the smallest *rms* error.

Figure 1 plots the probability density function of the raindrop diameter at two rain rates, 16 mm/hr and 50 mm/hr where various models are plotted, including Marshall and Palmer(MP) [4] and Joss et al. (J-T) [22], along with the gamma fitted in this study which shows the smallest rms error among the models comparison.

The drop density per unit volume, N_0, may be estimated by

$$N_0 = \frac{1}{T \cdot \Delta D \cdot A_0} \sum_{j=1}^{M} \frac{1}{v_j} \tag{4}$$

where T is the integration time, ΔD is the width between the minimum diameter to maximum diameter, A_0 is the measuring area, v_j is the terminal velocity of the specific droplet j, and M is the total number of drops passing through the measuring area within the integration time. In this study, the integration time was 60 seconds and measuring area A_0 was 92.9262 mm^2 set in distrometer. To further analyze the terminal velocity, the mean value of terminal velocity is related to the diameter, as plotted in Fig. 2. Also included is model proposed by Atlas and Ulbrich [1]. Consequently, we can find the relationship
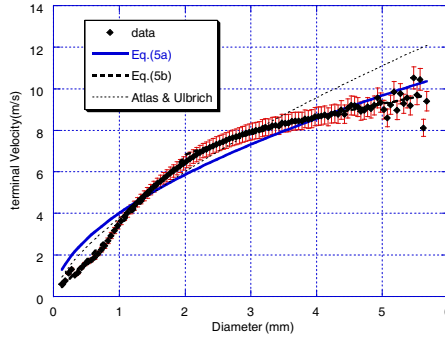
Figure 2. Measured terminal velocity and the curve fitting.

between the terminal velocity and the diameter which is given as

$$v = v(D) = 4.01 \cdot D^{0.546} \tag{5a}$$

$$v = v(D) = \begin{cases} 3.425 \cdot D^{0.976}, & D \le 2\,\text{mm} \\ 5.416 \cdot D^{0.335}, & D > 2\,\text{mm} \end{cases} \tag{5b}$$

From Eq. (3) and Eq. (4), the number density N_0 is estimated and subsequently the relationship between N_0 and rain rate R may be established. Again, using the power-law to fit considering the minimum *rms* for criteria, given as

$$N_0 = 318.64 R^{0.01671}. \tag{6}$$

3. PREDICATION OF RAIN ATTENUATION

The specific attenuation A due to rain using the DSD model was obtained from the relation

$$A = 4.343 \times 10^{-3} \int\limits_{0}^{\infty} N(D)Q(D)dD \quad (\text{dB/km}) \tag{7}$$

where Q is the extinction cross section.

The extinction coefficient is the function of the size and shape of rain drops, wavelength of EM wave, and the complex refractive index of water. In this study, we set the temperature was 20°C and the polarization was vertical polarization, then Mie scattering approximation and T-matrix method were used to estimate the extinction coefficient [21, 23]. It is known that the rain drop were not spherical, especially when the drop size is large, although it is generally reasonable to assume a spherical droplet for small drop size.

In what follows, we used rotationally symmetric ellipsoid and analyzed the droplet oblateness, followed by a discussion of its influence on rain attenuation. In this study, we will apply this method by assuming that rain drops are rotationally symmetric particles. First we analyze the oblateness of the rain drops. Fig. 3 is the side view of the rain drop with oblateness defined as ratio of short axis b to long axis a. Fig. 4 shows the mean oblateness as function of diameter of the measurement data. It is found that the mean oblateness decreased linearly from 1.0 to 0.8 when diameter increased from 1.0 to 6.0 mm. Fig. 4 shows the mean oblateness (OBL) versus the drop diameter, and the linear regression line. It can be seen that as the diameter increases, the oblateness decrease slowly. When the drop diameter is small, the oblateness approaches to 1, namely, a sphere.
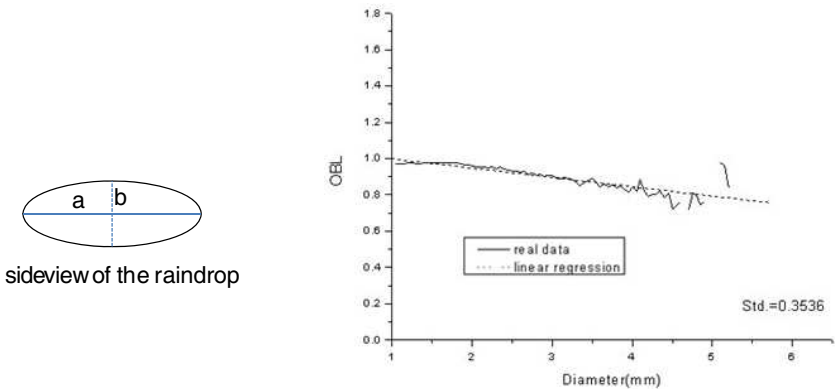
Figure 3. Definition of the oblateness b/a.

Figure 4. Mean oblateness versus the droplet diameter.

    In a rain volume, the particles usually are assumed to be randomly distributed within the volume, so that there are no coherent phase relationships between the fields scattered by the individual particles, thereby allowing the use of incoherent theory for computing the extinction (the absorption and the scattering) by a volume containing many particles. Additionally, the concentration of particles usually is small enough to support the assumption that shadowing of one particle by another may be ignored. Hence the total extinction cross-section of a given volume may be equal to the sum of the extinction cross sections of all the individual particles contained in that volume. Therefore, the attenuation due to rain can be estimated by calculating the extinction coefficient over all of the rain drops within the antenna beam volume.
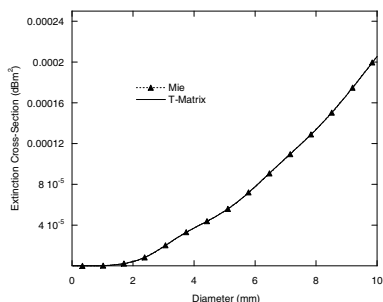
Figure 5. Extinction coefficient vs. droplet diameter computed by Mie theory and T-matrix method.
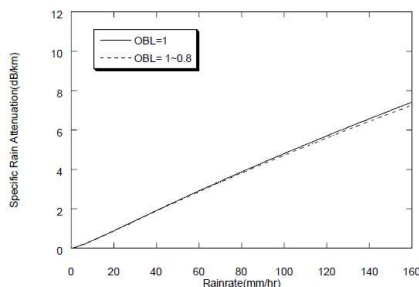
Figure 6. Specific rain attenuation in different oblateness conditions.

For purpose of computation, we set the frequency to 28 GHz in vertical polarization, the temperature at 20°C. Fig. 5 gives the extinction cross section as function of diameter computed by Mie theory and T-matrix method. It is found that extinction coefficient estimated by T-matrix method can match well with the ones estimated by Mie scattering approximation. We plot the specific rain attenuation estimated by T-matrix in Fig. 6. It is found the difference of the attenuation is 0.15 dB/km even when the rain rate is 160 mm/hr.

4. DATA ANALYSIS

To establish a prediction model based on Eq. (7), experiments were conducted to measure the rain attenuation using a 28 GHz continuous wave (CW) measurement system, rain gauges (optical and tipping bucket) and a 2D video distrometer in Taiwan. Two 34 dBi vertical polarization Cassigran antennas were employed for transmitting and receiving. The transmitter had +20 dBm power input to the antenna unit, while the receiver came with a 200 MHz IF signal output to the spectrum analyzer (HP8596E) through which the power level was automatically recorded in PC through a GPIB interface with 5 seconds integration time. For rain rate measurements, there are two types of gauges to record and provide cross reference with each other. The tipping bucket rain gauge has 0.1 mm sensitivity in which measured data were digitized and stored. The optical rain gauge (ORG-815) with 0.001 mm sensitivity was used to record cumulative data every 5 seconds. In addition, a 2D-vedio-distrometer for rain drop size measurement was devised. Then, a microwave link with line of sight (LOS) distance 0.6 km and elevation angle 1° was setup for rain
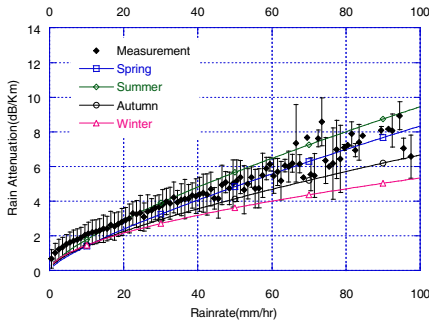
Figure 7. In situ measured rain attenuation at different seasons.
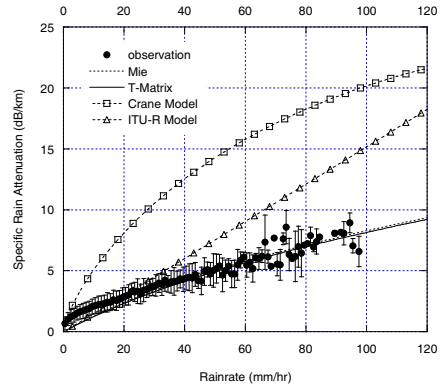
Figure 8. Specific rain attenuation about observation, proposed model, Crane model, and ITU-R model.

attenuation measurement. Fig. 7 shows the measured attenuation at various rain rates over two-year continuous measurements at different seasons. The data shows strong fluctuations over the rain rate larger than 100 mm/hr due to sparse data sets. To some degrees, the attenuation has dependence on season change. It seems that the group of autumn and winter and that of spring and summer have significant difference particularly at larger rain rates. The similarity within the same group implies the rainfall pattern. Next, we plotted model predictions against the measured data in Fig. 8. For this case, we can see that the extinction coefficient calculated by Mie and T-matrix does not make significant difference in predicting the rain attenuations. For the purpose of cross reference, the Crane model and ITU-R.P838 model were plotted, where we can see that both the two models notoriously overestimate the attenuation levels, as expected. It means that their predictions are not quite reliable in some specific areas. By taking DSD into account and using Eq. (7), the predictions are matching measurements quite well. Table 1 lists the RMS test from which it also confirms the above statement.

It should be noted that when applying the models the climate zone is critical to predict rain attenuation from the rainfall rate data. This is because rainfall types and so is DSD are dependent on climate environments even with the same rain rate. Table 2 lists $R_{0.01}$ (rainfall rate for 0.01% of an average year (mm/hr) values over Taiwan from north (Taipei) to south (Kaohsiung) according to 10 years weather data. The rainfall rates were well around 50 mm/hr. However, much

Table 1. Comparison between model predictions and measurements at 28 GHz terrestrial link.

Model	RMS
Mie Approximation	0.5975
T-matrix	0.6143
Crane Model	9.919
ITU-R Model	8.207

Table 2. The statistic of $R_{0.01}$ by hourly cumulative rainfall rate and those by models.

	Teipei	Chungli	Taichung	Kaohsiung
$R_{0.01}$	49 mm/hr	43 mm/hr	52 mm/hr	48 mm/hr
	ITU-R 837-2	Crane		
$R_{0.01}$	95 mm/hr	91.5 mm/hr		

higher values were adopted in either ITU-R837.2 or Crane models. Hence, it is not surprised to note a large error. In this paper, no attempt was made to modify the model according to the local parameters at this point, but should be of interest to do so in the future. Before closing the section, it is noted that shown in Fig. 7 and Fig. 8, due to presence of wetness on antenna surface, about 1 dB signal loss were observed in very light rain conditions.

5. CONCLUSION

Making use of the Gamma-distribution for DSD along with a two-year set of continuously measured data, and taking into account the extinction cross section estimated by Mie approximation and T-Matrix, a semi-empirical rain attenuation model was developed. To validate the model, we compared it with the measured data. For purpose of cross reference, we also compare the proposed model with Crane and ITU-R rain attenuation models. The RMS test shows that the proposed model has better performance to predicted rain attenuation. It means that both Crane and ITU-R models' predictions may not be quite reliable in some specific areas, since both the Crane and ITU-R model only concern about rain rate for the parameter and their $R_{0.01}$ values were too large for Taiwan area. It is found that specific rain attenuation in spring and summer is higher than it is in autumn and winter. The difference between different seasons is more significant than different

years. It means that seasonal effect cannot be ignored when analyze
the rain attenuation in specific seasons.

REFERENCES

1. Atlas, D. and C. W. Ulbrich, "Path- and area-integrated rainfall measurement by microwave attenuation in the 1–3 cm band," *J. Appl. Meteor.,* Vol. 16, 1322–1331, 1977.

2. Freeman, R. L., *Radio System Design for Telecommunications*, 2nd Edition, Wiley, 1997.

3. Crane, R. K., *Electromagnetic Wave Propagation Through Rain*, Wiley, 1996.

4. Marshall, J. S. and W. M. Palmer, "The distribution of raindrops with size," *J. Meteor.,* Vol. 5, 165–166, 1948.

5. Jiang, H., M. Sano, and M. Sekine, "Weibull raindrop-size distribution and its application to rain attenuation," *IEE Proc. — Microw. Antennas Propag.*, Vol. 144, 197–200, 1997.

6. Timothy, K. I. and S. K. Sarkar, "Generalised mathematical model for raindrop size distribution (RSD) for application in radiowave propagation and meteorological studies," *Electro. Lett.*, Vol. 33, 895–897, 1997.

7. Maitra, A., "Three-parameter raindrop size distribution modeling at a tropical location," *Electro. Lett.*, Vol. 36, 906–907, 2000.

8. Yeo, T. S., P. S. Kooi., M. S. Leong, and L. W. Li, "Tropical raindrop size distribution for the prediction of rain attenuation of microwaves in the 10–40 GHz band," *IEEE Trans. Antenna and Propagation*, Vol. 49, 80–83, 2001.

9. Timothy, K. I., J. T. Ong, and E. B. L. Choo, "Raindrop size distribution using method of moments for terrestrial and satellite communication applications in Singapore," *IEEE Trans. Antenna and Propagation*, Vol. 50, 1420–1424, 2002.

10. Chu, C. Y. and K. S. Chen, "Effects of rain fading on the efficiency of the Ka-band LMDS system in the Taiwan area," *IEEE Trans. Vehicular Technology*, Vol. 54, No. 1, 9–19, 2005.

11. Zhang, W. and N. Moayeri, "Power-law parameters of rain specific attenuation," *IEEE 802.16 Broadband Wireless Access Working Group*, IEEE 802.16cc-99/24.

12. Maitra, A., "Rain attenuation modeling from measurements of rain drop size distribution in the Indian region," *IEEE Antenna and Wireless Propagation Letters*, Vol. 3, 180–181, 2004.

13. Townsend, A. J., R. J. Watson, and D. D. Hodge, "Analysis

of the variability in the raindrop size distribution and its effect on attenuation at 20–40 GHz," *IEEE Antenna and Wireless Propagation Letters*, Vol. 8, 1210–1213, 2009.

14. Lee, C. H., G. Lee, I. Zawadzki, and K.-E. Kim, "A preliminary analysis of spatial variability of raindrop size distributions during stratiform rain events," *J. Appl. Meteor. Climate*, Vol. 48, No. 2, 270–283, 2009, doi:10.1175/2008JAMC1877.1.

15. Berne, A., J. Jaffrain, and M. Schleiss, "Scaling analysis of the DSD variability at small spatial scales," *Proceedings of the VIth European Conference on Radar in Meteorology and Hydrology*, 259–264, National Meteorological Administration, Sibiu, Romania, 2010.

16. Olsen, R. L., D. V. Roger, and D. B. Hodge, "The aR^b relation in the calculation of rain attenuation," *IEEE Trans. Antenna and Propagation*, Vol. 26, 1978.

17. Li, L.-W., P. S. Kooi, M. S. Leong, M. Z. Gao, and T. S. Yeo, "Microwave attenuation by realistically distorted raindrops: Part I — Theory," *IEEE Trans. Antenna and Propagation*, Vol. 43, 811–822, 1995.

18. Li, L.-W., P. S. Kooi, M. S. Leong, M. Z. Gao, and T. S. Yeo, "Microwave attenuation by realistically distorted raindrops: Part II — Predictions," *IEEE Trans. Antenna and Propagation*, Vol. 43, 823–828, 1995.

19. Lin, D.-P. and H.-Y. Chen, "Volume integral equation solution of extinction cross section by rain drops in the range 0.6–100 GHz," *IEEE Trans. Antenna and Propagation*, Vol. 49, 494–499, 2001.

20. Tseng, C. H., K. S. Chen, J. C. Shi, and C. Y. Chu, "Prediction of Ka-band terrestrial rain attenuation using 2-year rain drop size distribution measurements in Northern Taiwan," *Journal of Electromagnetic Waves and Applications*, Vol. 19, No. 13, 1833–1841, 2005.

21. Mishchenko, M. I., L. D. Travis, and A. A. Lacis, *Scattering, Absorption, and Emission of Light by Small Particles*, Cambridge University, 2002.

22. Joss, J., J. C. Thams, and A. Waldvogel, "The variation of raindrop-size distribution at Locarno," *Proceedings of International Conference on Cloud Physics*, 369–373, 1967.

23. Sadiku, N. O., *Numerical Techniques in Electromagnetics*, CRC, 1992.